

Video Article

***In-situ* Tapering of Chalcogenide Fiber for Mid-infrared Supercontinuum Generation**

Charles W. Rudy¹, Alireza Marandi¹, Konstantin L. Vodopyanov¹, Robert L. Byer¹

¹Edward L. Ginzton Laboratory, Stanford University

Correspondence to: Charles W. Rudy at cwrudy@stanford.edu

URL: <https://www.jove.com/video/50518>

DOI: [doi:10.3791/50518](https://doi.org/10.3791/50518)

Keywords: Physics, Issue 75, Engineering, Photonics, Optics, infrared spectra, nonlinear optics, optical fibers, optical waveguides, wave propagation (optics), fiber optics, infrared optics, fiber tapering, chalcogenide, supercontinuum generation, mid-infrared, *in-situ*, frequency comb, scanning electron microscopy, SEM

Date Published: 5/27/2013

Citation: Rudy, C.W., Marandi, A., Vodopyanov, K.L., Byer, R.L. *In-situ* Tapering of Chalcogenide Fiber for Mid-infrared Supercontinuum Generation. *J. Vis. Exp.* (75), e50518, doi:10.3791/50518 (2013).

Abstract

Supercontinuum generation (SCG) in a tapered chalcogenide fiber is desirable for broadening mid-infrared (or mid-IR, roughly the 2-20 μm wavelength range) frequency combs^{1,2} for applications such as molecular fingerprinting,³ trace gas detection,⁴ laser-driven particle acceleration,⁵ and x-ray production via high harmonic generation.⁶ Achieving efficient SCG in a tapered optical fiber requires precise control of the group velocity dispersion (GVD) and the temporal properties of the optical pulses at the beginning of the fiber,⁷ which depend strongly on the geometry of the taper.⁸ Due to variations in the tapering setup and procedure for successive SCG experiments-such as fiber length, tapering environment temperature, or power coupled into the fiber, *in-situ* spectral monitoring of the SCG is necessary to optimize the output spectrum for a single experiment.

In-situ fiber tapering for SCG consists of coupling the pump source through the fiber to be tapered to a spectral measurement device. The fiber is then tapered while the spectral measurement signal is observed in real-time. When the signal reaches its peak, the tapering is stopped. The *in-situ* tapering procedure allows for generation of a stable, octave-spanning, mid-IR frequency comb from the sub harmonic of a commercially available near-IR frequency comb.⁹ This method lowers cost due to the reduction in time and materials required to fabricate an optimal taper with a waist length of only 2 mm.

The *in-situ* tapering technique can be extended to optimizing microstructured optical fiber (MOF) for SCG¹⁰ or tuning of the passband of MOFs,¹¹ optimizing tapered fiber pairs for fused fiber couplers¹² and wavelength division multiplexers (WDMs),¹³ or modifying dispersion compensation for compression or stretching of optical pulses.¹⁴⁻¹⁶

Video Link

The video component of this article can be found at <https://www.jove.com/video/50518/>

Introduction

After being first produced in the visible wavelength range^{1,7} SCG sources have shifted towards the mid-IR, largely driven by applications in spectroscopy.^{3,4} Chalcogenide fibers, which include sulfides, selenides, and tellurides, have been a popular material for the mid-IR due to their low propagation loss and high nonlinearity,¹⁸ less than 100 dB/km¹⁹ and ~200 times that of silica for As₂S₃,²⁰ respectively. However, the zero GVD wavelength of most chalcogenides is located in the mid-IR, beyond the center wavelength of the majority of available ultrafast pump sources, making SCG challenging in a bulk material or a standard single mode chalcogenide fiber. Waveguide dispersion can be used to modify the zero GVD point for SCG.⁷ Methods for introducing strong waveguide dispersion include fiber tapering,^{8,21} using microstructured fibers,²²⁻²⁴ or even a combination of the two.¹⁰ By shifting the zero GVD wavelength below the pump wavelength, the pump will experience anomalous dispersion in the fiber. In the anomalous dispersion regime, soliton formation occurs through balancing the nonlinear chirp caused by self phase modulation and the linear chirp caused by GVD. For a femtosecond pump source, spectral broadening is usually dominated by soliton fission or pulse breaking, which occurs after an initial temporal compression as the pulse propagates along the fiber.⁷ In the case of fiber tapering, calculating the total GVD-including both material and waveguide dispersion-can provide an approximation of the final taper diameter needed to produce a significantly broadened spectrum. Due to SCG's strong dependence on GVD and fluctuations between experimental trials, including changes to the fiber length before the tapered region and coupling of the pump to the fiber, the calculated approximation is not sufficient for achieving an optimized taper in a single trial. Spectral monitoring allows for these variations in experimental setup to be observed and accounted for in *in-situ* tapering.

Moreover, generating an efficient supercontinuum (SC) in a short tapered fiber reduces the amount of nonlinear noise amplification preserving the coherence of the SCG and the frequency comb properties of the pump source.²⁵⁻²⁷ Proper dispersion management, and therefore the necessity of *in-situ* tapering, becomes even more critical when the fiber length is short, as the SCG tolerance scales with length.

The *in-situ* tapering setup begins with the pump source, which is the subharmonic of a mode-locked Er-doped fiber laser,⁹ coupled into the core of the As₂S₃ fiber that will be tapered. The output of the fiber is then coupled to a device that characterizes the spectral profile. In the experiment, a InSb detector after a monochromator with ~20 nm of resolution is used to monitor a portion of the output spectrum where there is initially a very low signal from the pump source (at ~3.9 μ m) so that the fiber may be monitored while tapering. When the fiber is tapered and the spectrum broadens, the spectral measurement signal increases as the dispersion is optimized for the individual experiment. By monitoring the spectrum during the tapering procedure, tapering can be stopped at the moment when the spectral broadening has been maximized. *In-situ* tapering allows for optimized dispersion management for efficient SCG in a single fiber taper. Tapering with a static, narrow heat zone produces a short fiber taper waist,²⁸ which allows for low-noise SCG. Together, *in-situ* static tapering can enable coherent, low-noise, octave-spanning SCG in the mid-IR.

Protocol

1. Tapering Setup Fabrication (See Assembled Setup in Figure 1)

- Secure the motorized linear stages on the breadboard (roughly centered) so that the stages are in contact and will translate towards and away from one another
- Prepare and place the fiber mounts
 - Attach two optical posts to the motorized linear stage plates (one each) using the holes closest to each other.
 - Attach the bare optical fiber mounts to the tops of the posts. Make sure that the v-grooves for the fiber are aligned. (Note: The height of the bare optical fiber mounts will roughly be the beam height of the system. Choose the future post and pedestal heights accordingly.)
- Prepare and place the input and output coupling elements
 - Attach the linear translation stages to the motorized linear stages (one for the input and one for the output side) with the adapter plates.
 - Place the AR coated ZnSe input coupling lens (mounted in an optical mount with x and y translation on a pedestal) on the input translation stage. Choose a focal length that gives optimal coupling from the pump source to the core of the fiber. Make sure the center of the lens is at the same height as the v-grooves of the fiber clamps.
 - Place the uncoated ZnSe output coupling lens (mounted in an optical mount with x and y translation on a pedestal) on the output translation stage. Make sure the center of the lens is at the same height as the v-groove.
- Prepare and place the heating element (as shown in Figure 2)
 - Machine the aluminum block to desired dimensions (~6 mm x 25.4 mm x 17.5 mm) with holes for the fiber (with a slit for inserting and removing the fiber) and for monitoring the fiber temperature, holes for the cartridge heaters, and 8/32 tapped holes on top and bottom for mounting and securing the cartridge heaters.
 - Insert the cartridge heaters to the proper holes of the aluminum block and secure them with 8/32 set screws.
 - Attach a ceramic post to the top 8/32 set screw for thermal isolation.
 - Attach an optical post to the ceramic post and use a right angle post clamp with an additional optical post to secure the heater to the XYZ linear stage.
 - Secure the XYZ linear stage to the breadboard so that the hole for the As₂S₃ fiber in the aluminum heater can be centered with the v-grooves of the fiber clamps.
 - Translate the aluminum heater with the XYZ linear stage so that the heater is no longer near the bare optical fiber clamps, allowing the fiber to be secured without obstruction.

2. Chalcogenide Fiber Preparation

- Soak a desired length of the jacketed As₂S₃ fiber (must be longer than 8.5 cm—the length of jacketed fiber needed for each fiber taper) in acetone for about 10 min or until the jacket becomes soft. (Use the appropriate solvent for the jacket if using a different fiber).
- Gently remove the softened jacket with a KimWipe, removing a section no longer than 5 cm at a time.
- Clean the bare fiber with isopropanol on a KimWipe.
- Use the beavertail cleaver to cleave one end of the As₂S₃ fiber. Image the discarded fiber tip to inspect cleave quality.
- Measure and break at least a 6.35-cm length piece of the fiber. This fiber length must be ~2 cm longer than the length needed for the fiber to barely stick out of the fiber clamps.
- Use the beavertail cleaver to cleave the second end of the fiber. Image the discarded fiber tip to inspect cleave quality. Avoid contact with the first cleaved end of fiber.
- Place the fiber in the fiber clamps of the tapering setup. Avoid touching the center of the fiber (where the fiber will be heated).

3. In-situ Fiber Tapering Procedure

- Couple the mid-IR pump source to the fundamental mode of the fiber with the AR coated ZnSe lens ($f = 12.7$ mm). Use the uncoated ZnSe lens ($f = 20$ mm) to image the output facet of the fiber with the Pyrocam to ensure the power is mostly in the fundamental mode. Make sure that the pump beam is propagating along the axis of the fiber. If it is not, the coupling will change once the motorized stages begin to move.
- Place a chopper in front of the pump source. (This step is needed for AC coupled detectors).
 - Couple the output of the fiber through the monochromator and to the InSb detector using the uncoated CaF₂ lenses ($f = 20$ mm) before and after the monochromator.
 - Rotate the grating of the monochromator to allow the long wavelength side of the spectrum to pass through the monochromator until the transmitted signal is barely above the noise floor (at ~3.9 μ m). Instead of filtering with the monochromator (steps 3.2.2 and

3.2.3), an appropriate optical filter can be used to measure the power in detectable wavelengths longer than the longest measureable wavelength content of the pump.

3. Translate the aluminum heater until the fiber slips through the slit and is centered in the aluminum heater's fiber hole.
4. Place the RTD sensor level with one of the cartridge heaters. Gently press the RTD sensor against the aluminum heater so that it is fully in contact with the block as shown in **Figure 2**. If the RTD is not in contact with the heater correctly (or not in a repeatable fashion), the temperature of the block will be unknown and cause the fiber to break during tapering. Make sure that the signal to the monochromator has not decreased.
 1. A small RTD can be placed inside the other hole of the heater block to monitor the temperature in the hole. (Optional)
5. Use the digital microscope to image the fiber in the heater block to allow for monitoring of the fiber during the tapering process. (Optional)
6. Cover the setup with a box (with holes for the input and output beams) to reduce airflow and allow for stable tapering temperature.
7. With the RTD and cartridge heaters connected, turn on the temperature controller. Set the temperature to $\sim 200^\circ\text{C}$, where the fiber begins to soften (the exact temperature will depend on the dimensions of the heater, the environment temperature, and air flow around the fiber).
8. Once the temperature is stable around the set point, start the Labview program that translates the motorized stages away from one another at $\sim 10\ \mu\text{m}/\text{sec}$ in each direction.
9. Monitor the signal of the InSb detector, which is the spectral measurement signal. Once the detector signal reaches its maximum value (be careful not to saturate the detector), stop the motorized stages and turn off the cartridge heaters (temperature controller).
10. Wait for $\sim 10\ \text{min}$ for the fiber to solidify (the detector signal will decrease a little during this process, most likely due to the temperature dependence of the refractive index or thermal contraction).
11. Translate the heater block along the fiber towards a fiber clamp where the fiber is untapered. Then translate the heater block away from the fiber using the slit in the heater block to allow the fiber to pass.
12. Characterize the SCG through spectral measurements with the monochromator. An InAs filter may be needed to accurately measure the long wavelength portion of the spectrum.
13. Remove the fiber if desired.

Representative Results

After successful completion of the *in-situ* tapering procedure, the pump spectrum broadened to cover from 2.2 to $5\ \mu\text{m}$ (at $\sim 40\ \text{dB}$ below the peak), as seen in **Figure 3**. The pump pulse energy in the As_2S_3 fiber was $\sim 250\ \text{pJ}$ with an initial pulse length under 100 fsec. The short length of the tapered waist, $\sim 2.1\ \text{mm}$, allows for generation of a broadband, coherent SC. This preserves the frequency comb properties of the pump source. More information about the frequency comb and other properties of the SCG may be found in ¹.

The resulting tapered fiber waist from the single mode As_2S_3 fiber (originally $7\ \mu\text{m}$ core diameter, $160\ \mu\text{m}$ cladding diameter, and 0.2 NA) is shown in an SEM image in **Figure 4**. At a diameter of $\sim 2.3\ \mu\text{m}$, the taper waist is too small to be observable by eye when in the setup, but it can be observed through diffraction of a light source. The tapered waist will be approximately as long as the effective heat zone of the heater block. Static tapering generates a long, exponential transition region from the untapered fiber to the tapered fiber waist that occupies the remaining $\sim 16\ \text{mm}$ of the pulling length.

As the fiber is being tapered, the detected spectral measurement signal resembles **Figure 5**. This signal should remain roughly constant until spectral broadening in the fiber begins to occur when the GVD becomes close to optimal. The signal increases to a peak at a pulling length of $\sim 18\ \text{mm}$ and quickly begins to fall as the GVD passes the optimum point. The 3-dB width of the peak in the spectral measurement signal is only 252 nm and the 10-dB width is 572 nm, which demonstrates the sensitivity to the tapered fiber diameter and emphasizes the necessity for *in-situ* tapering.

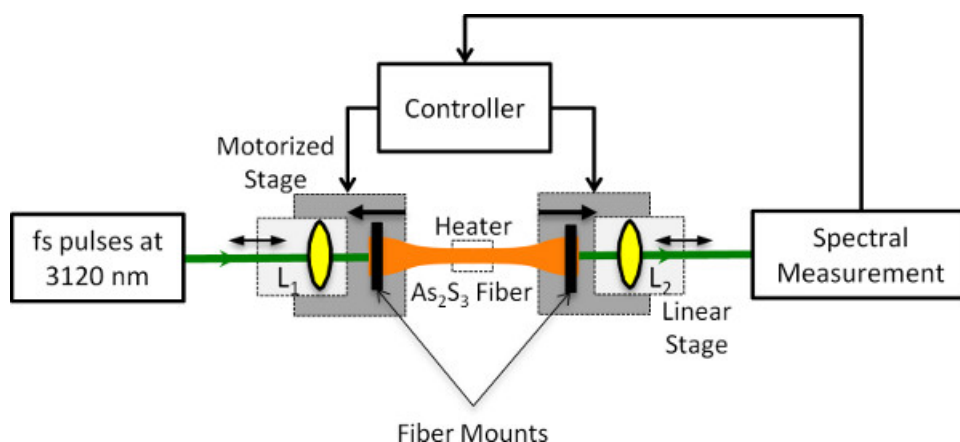


Figure 1. *In-situ* Fiber Tapering Setup. The fs pump source is coupled into the As_2S_3 fiber with lens L_1 by optimizing L_1 's linear stage position (shown in light gray) and the XY position of the lens mount (not shown in the figure). The output of the fiber is coupled to the spectral measurement device with L_2 optimized by a linear stage. The motorized stages (shown in dark gray) pull the fiber away from the central heater and stop when the spectral measurement value is maximized.

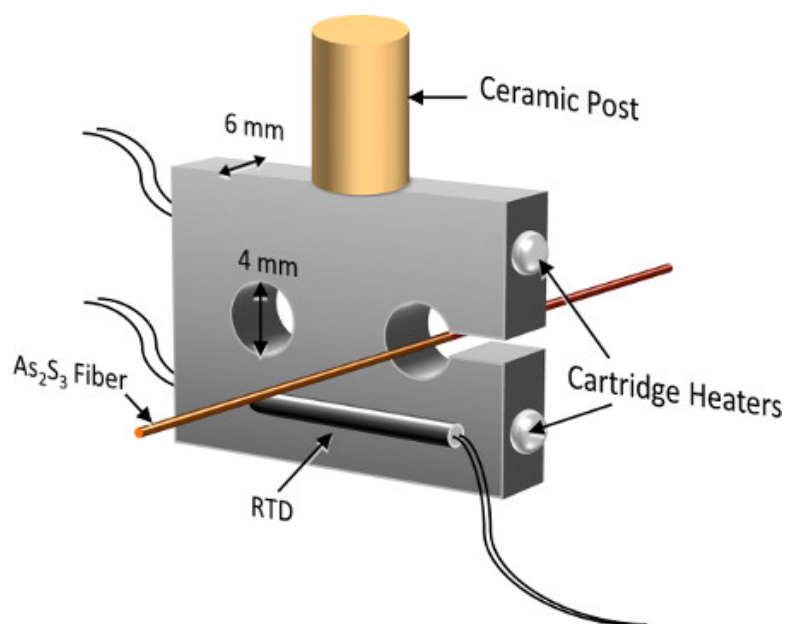


Figure 2. Aluminum Heater Block. The heater block is ~6 mm thick with two 4-mm holes (one for the fiber and one to monitor the approximate temperature of the fiber). A small slit is cut in the block to allow for insertion and removal of the fiber. The block is 2.54 cm long, which is just long enough to fit the entire heating element of the cartridge heaters. A ceramic post (attached with an 8/32 set screw) provides thermal isolation. The RTD sensor is placed in contact with the heater block and level with a cartridge heater to provide the quickest feedback loop possible. The height of the block-not an important dimension as long as there is room for the cartridge heaters, 4-mm holes for the fiber, and taps to mount the heater block-is ~1.75 cm.

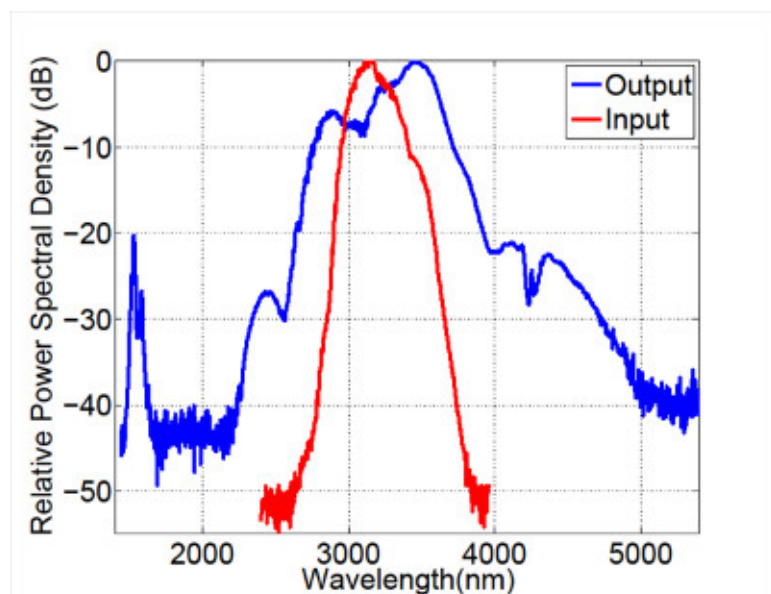


Figure 3. SCG Spectrum. The normalized spectra of the input (pump) and output (SCG) are shown. The generated bandwidth of the output is ~3 times broader than the input in frequency units at 40 dB below the peak. The dip in the output spectrum around 4.2 μm corresponds to CO₂ absorption in the atmosphere.

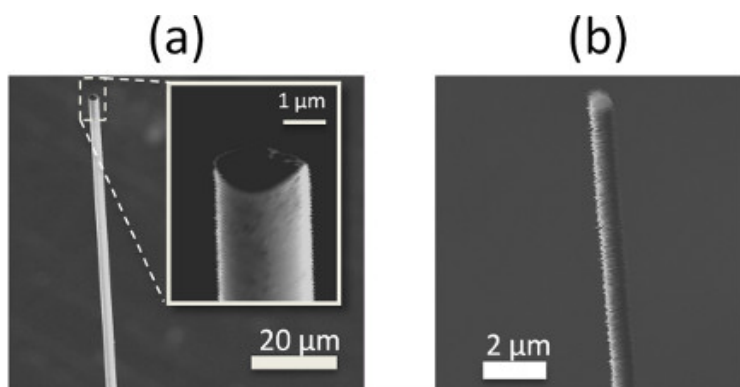


Figure 4. SEM Images of Tapered As_2S_3 Fiber. Examples of the tapered As_2S_3 fibers are shown in (a) and (b) (purposely broken after tapering for SEM imaging). (a) The SEM image of an As_2S_3 fiber tapered to approximately the diameter for optimum SCG, $\sim 2.3 \mu\text{m}$. (b) An SEM image of an As_2S_3 fiber tapered demonstrates the smallest tapered diameter created with the setup, $\sim 760 \text{ nm}$.

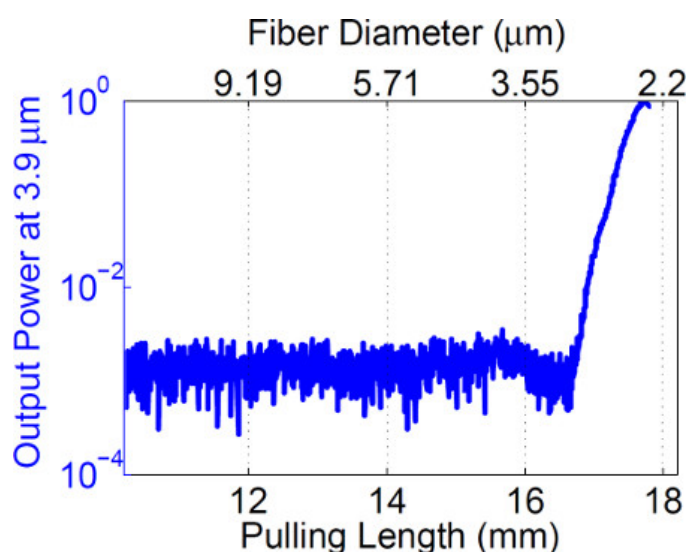


Figure 5. Spectral Measurement Signal vs. Pulling Length. The normalized output power after the monochromator, set stationary at $3.9 \mu\text{m}$, is shown for a single fiber taper experiment. The output power begins to dramatically increase after $\sim 17 \text{ mm}$ of pulling length. The maximum signal occurs close to 18 mm of pulling length, corresponding to a fiber diameter of $\sim 2.3 \mu\text{m}$. The motorized stages were stopped shortly after this peak was reached.

Discussion

We have demonstrated a novel fiber tapering procedure and verified its validity by performing SCG in the mid-IR. To the best of our knowledge, the alternative method for this application is based on determining the fiber pulling length required to create a tapered fiber diameter that adds enough waveguide dispersion to optimize SCG in the fiber taper through calculation; however, since the pulling length needed to maximize the spectral broadening for a specific length of fiber varies for each experiment, this calculated value is only an approximation. The alternative method then requires fiber tapers to be created and tested one after another until a desired taper is found. By being able to monitor the spectral profile of the SCG and use it as the criterion for stopping the tapering process, we have optimized the output of a single fiber taper to achieve substantial broadening in a short taper. This greatly reduces the cost and time needed to generate a useful fiber taper.

The most common failure is breakage of the fiber during the tapering procedure. Breaks are usually caused by improperly setting the temperature of the heater block. If the temperature is too low, the fiber will break due to high tension. If the temperature is too high, surface crystallization,²⁹ which generates cracks in the surface of the fiber that easily propagate under tension, can produce a break in the fiber. Of the two, the more frequent mode of failure was overheating the fiber, usually from not placing the RTD sensor in the proper position. A fiber break is easily detectable as the spectral measurement signal will suddenly drop to the noise floor.

Further improvements to the setup are possible. For instance, permanently attaching the RTD sensor to the heater block would allow for a more repeatable tapering temperature, eliminating the most common mode of failure. Also, removing moisture from the tapering setup by purging the setup with dry N_2 may help avoid breakages during tapering. Removing a successful fiber taper has been accomplished, but a reproducible procedure has not yet been developed. Coating the As_2S_3 fiber with a thick, protective, low index, low loss, cladding material could improve the mechanical stability of the fiber and allow for easier handling of the tapered fiber. Using alternative methods for monitoring the spectrum, such as using a long-wavelength pass filter that transmits on the long-wavelength side of the pump source, could simplify the detection scheme. There are several optional modifications that may be able to expand the usefulness of the current *in-situ* tapering setup. The dimensions of the aluminum heater block can be altered to change the length of the tapered region. Dynamic tapering, which consists of moving the heating

element with respect to the fiber during tapering (flame brushing) and/or moving the stages at different velocities, can also be done with *in-situ* monitoring. This would allow for different tapered fiber profiles to be created. The total dispersion experienced by the pump source would then depend on the profile created. Also, replacing the heating element with a high temperature heater would permit fibers with higher melting points to be tapered.

Although not yet demonstrated, the *in-situ* fiber tapering technique can be applied to other fiber-based devices that are produced through fiber tapering. Slight tapering in MOFs can fine tune the dispersion of the fiber for efficient SCG.¹⁰ By using a broadband source that covers the passband of an MOF (perhaps an SCG based source), the passband, which scales with the dimension size of the microstructuring, can be blue-shifted using *in-situ* fiber tapering.¹¹ Additionally, a broadband source can be used to characterize fiber components, such as fiber couplers¹² and WDMs,¹³ fabricated through fiber tapering during production to better meet specifications. *In-situ* fiber tapering can be adapted to optimize the results of most fiber tapering experiments.

Disclosures

A United States provisional patent has been filed protecting the technology disclosed in this article.

Acknowledgements

The authors would like to thank G. Shambat, C. Phillips, K. Aghaei for invaluable discussions, F. Afshinmanesh for SEM images, T. Marvdashti for experimental support, and M.F. Churbanov and G.E. Snopatin from the Institute of Chemistry of High-Purity Substances and V.G. Plotnichenko and E.M. Dianov from the Fiber Optics Research Center of the Russian Academy of Sciences for providing the As₂S₃ fiber. We also are grateful for support from the Office of Naval Research, NASA, the Air Force Office of Scientific Research, Agilent, and the Joint Technologies Office.

References

1. Marandi, A., Rudy, C.W., Plotnichenko, V.G., Dianov, E.M., Vodopyanov, K.L., & Byer, R.L. Mid-infrared supercontinuum generation in tapered chalcogenide fiber for producing octave-spanning frequency comb around 3 μm . *Optics Express*. **20**, 24218-24225 (2012).
2. Schliesser, A., Picque, N., & Hansch, T.W. Mid-infrared frequency combs. *Nature Photonics*. **6**, 440-449 (2012).
3. Diddams, S.A., Hollberg, L., & Mbele V. Molecular fingerprinting with the resolved modes of a femtosecond laser frequency comb. *Nature*. **445**, 627-630 (2007).
4. Thorpe, M.J., Balslev-Clausen, D., Kirchner, M.S., & Ye, J. Cavity-enhanced optical frequency comb spectroscopy: application to human breath analysis. *Optics Express*. **16**, 2387-2397 (2008).
5. Sears, C.M.S., Colby, E., England, R.J., Ischebeck, R., McGuinness, C., Nelson, J., Noble, R., Siemann, R.H., Spencer, J., Walz, D., Plettner, T., & Byer, R.L. Phase stable net acceleration of electrons from a two-stage optical accelerator. *Physical Review Letters*. **11**, 101301 (2008).
6. Popmintchev, T., Chen, M.C., Arpin, P., Murnane, M.M., & Kapteyn, H.C. The attosecond nonlinear optics of bright coherent X-ray generation. *Nature Photonics*. **4**, 822-832 (2010).
7. Dudley, J.M. & Taylor, J.R. *Supercontinuum generation in optical fibers*. Cambridge University Press, (2010).
8. Birks, T.A., Wadsworth, W.J., & Russell, P.S.J. Supercontinuum generation in tapered fibers. *Optics Letters*. **25**, 1415-1417 (2000).
9. Leindecker, N., Marandi, A., Byer, R.L., & Vodopyanov, K.L. Broadband degenerate OPO for mid-infrared frequency comb generation. *Optics Express*. **19**, 6296-6302 (2011).
10. Liao, M., Yan, X., Gao, W., Duan, Z., Qin, G., Suzuki, T., & Ohishi, Y. Five-order SRSs and supercontinuum generation from a tapered tellurite microstructured fiber with longitudinally varying dispersion. *Optics Express*. **19**, 15389-15396 (2011).
11. Mägi, E.C., Steinvurzel, P., & Eggleton, B.J. Tapered photonic crystal fibers. *Optics Express*. **12**, 776-784 (2004).
12. Ozeki, T. & Kawasaki, B.S. Optical directional coupler using tapered sections in multimode fibers. *Applied Physics Letters*. **28**, 528-529 (1976).
13. Yataki, M.S., Payne, D.N., & Varnahm, M.P. All-fibre wavelength filters using concatenated fused-taper couplers. *Electronic Letters*. **21**, 248-249 (1985).
14. Chandalia, J.K., Eggleton, B.J., Windeler, R.S., Kosinski, S.G., Liu, X., & Xu, C. Adiabatic coupling in tapered air-silica microstructured optical fiber. *IEEE Photonics Technology Letters*. **13**, 52-54 (2001).
15. Mora, J., Díez, A., Andréz, Fonjallaz, P.Y., & Popov, M. Tunable dispersion compensator based on a fiber Bragg grating written in a tapered fiber. *IEEE Photonics Technology Letters*. **16**, 2631-2633 (2004).
16. Rusu, M., Herda, R., Kivistö, S., & Okhotnikov, O.G. Fiber taper for dispersion management in a mode-locked ytterbium fiber laser. *Optics Letters*. **31**, 2257-2259 (2006).
17. Alfano, R.R. & Shapiro, S.L. Emission in the region 4000 to 7000 Å via four-photon coupling in glass. *Physical Review Letters*. **24**, 584-587 (1970).
18. Eggleton, B.J., Luther-Davies, B., & Richardson, K. Chalcogenide photonics. *Nature Photonics*. **5**, 141148 (2011).
19. Snopatin, G.E., Shiryaev, V.S., Plotnichenko, V.G., Dianov, E.M., & Churbanov, M.F. High-purity chalcogenide glasses for fiber optics. *Inorganic Materials*. **45**, 1439-1460 (2009).
20. Harbold, J.M., Ilday, F.O., Wise, F.W., Sanghera, J.S., Nguyen, V.Q., Shaw, L.B., & Aggarwal, I.D. Highly nonlinear As-S-Se glasses for all-optical switching. *Optics Letters*. **27**, 119-121 (2002).
21. Hudson, D.D., Dekker, S.A., Magi, E.C., Judge, A.C., Jackson, S.D., Li, E., Sanghera, J.S., Shaw, L.B., Aggarwal, I.D., & Eggleton, B.J. Octave spanning supercontinuum in an As₂S₃ taper using ultralow pump pulse energy. *Optics Letters*. **36**, 1122-1124 (2011).
22. Domachuk, P., Wolchover, N.A., Cronin-Golomb, M., Wang, A., George, A.K., Cordeiro, C.M.B., Knight, J.C., & Omenetto, F.G. Over 4000 nm bandwidth of mid-IR supercontinuum generation in sub-centimeter segments of highly nonlinear tellurite PCFs. *Optics Express*. **6**, 7161-7168 (2008).

23. Hu, J., Menyuk, C.R., Shaw, L.B., Sanghera, J.S., & Aggarwal, I.D. Maximizing the bandwidth of supercontinuum generation in As₂Se₃ chalcogenide fibers. *Optics Express*. **18**, 6722-6739 (2010).
24. El-Amraoui, M., Fatome, J., Jules, J.C., Kibler, B., Gadret, G., Fortier, C., Smektala, F., Skripatchev, I., Polacchini, C.F., Messaddeq, Y., Troles, J., Brilland, L., Szpulak, M., & Renversez, G. Strong infrared spectral broadening in low-loss As-S chalcogenide suspended core microstructured optical fibers. *Optics Express*. **18**, 4547-4556 (2010).
25. Marandi, A., Leindecker, N., Byer, R.L., & Vodopyanov, K.L. Coherence properties of a broadband femtosecond mid-IR optical parametric oscillator operating at degeneracy. *Optics Express*. **20**, 7255-7262 (2012).
26. Dudley, J.M. & Coen, S. Coherence properties of supercontinuum spectra generated in photonic crystal and tapered optical fibers. *Optics Letters*. **27**, 1180-1182 (2002).
27. Corwin, K.L., Newbury, N.R., Dudley, J.M., Coen, S., Diddams, S.A., Weber, K., & Windeler, R.S. Fundamental noise limitations to supercontinuum generation in microstructure fiber. *Physical Review Letters*. **90**, 113904 (2003).
28. Birks, T.A. & Li, Y.W. The shape of fiber tapers. *Journal of Lightwave Technology*. **10**, 432-438 (1992).
29. Churbanov, M.F. High-purity chalcogenide glasses as materials for fiber optics. *Journal of Non-Crystalline Solids*. **184**, 25-29 (1995).